Inorganic Chemistry

ARTICLE

pubs.acs.org/IC

NMR Studies of Models Having the Pt(d(GpG)) 17-Membered Macrocyclic Ring Formed in DNA by Platinum Anticancer Drugs: Pt Complexes with Bulky Chiral Diamine Ligands

Jamil S. Saad,[*,†,‡] Michele Benedetti,[§,∥] Giovanni Natile,[§] and Luigi G. Marzilli[*,†]

[†]Department of Chemistry, Louisiana State University, Baton Rouge, Louisiana 70803, United States and Department of Chemistry, Emory University, Atlanta, Georgia 30322, United States

[§]Dipartimento Farmaco-Chimico, Università di Bari, Via E. Orabona, 4, 70125 Bari, Italy

Supporting Information

ABSTRACT: The highly distorted Pt(d(G*pG*)) (G* = N7-platinated G) 17-membered macrocyclic ring formed by cisplatin anticancer drug binding to DNA alters the structure of the G*G* base pair steps, canting one base, and increases dynamic motion, complicating solution structural studies. However, the ring appears to favor the HH1 conformation (HH1 denotes head-to-head guanine bases, 1 denotes the normal direction of backbone propagation). Compared to cisplatin, analogues with NH groups in the carrier ligand replaced by bulky N-alkyl groups are more toxic and less active and form less dynamic adducts. To examine the molecular origins for the biological effects of steric bulk, we evaluate **Me$_4$DAB**Pt(d(G*pG*)) models; the bulk and chirality of **Me$_4$DAB** (*N*,*N*,*N*′,*N*′-tetramethyl-2,3-diaminobutane with *S*,*S* or *R*,*R* configurations at the chelate ring carbons) impede dynamic motion and enhance the utility of NMR methods for identifying and characterizing conformers. Unlike past studies of adducts with such bulky carrier ligands, in which no HH conformer was found, the **Me$_4$DAB**Pt(d(G*pG*)) adducts did form the HH1 conformer, providing compelling evidence that the sugar−phosphate backbone can impose constraints sufficient to overcome the alkyl-group steric effects. The HH1 conformer exhibits no significant canting. The (*S*,*S*)-**Me$_4$DAB**Pt(d(G*pG*)) adduct has the least amount of the "normal" HH1 conformer and the greatest amount of the ΔHT1 conformer (ΔHT1 = head-to-tail G* bases with Δ chirality) ever observed (88% under some conditions). Thus, our results lead us to hypothesize that the low activity and high toxicity of analogues of cisplatin having carrier ligands with N-alkyl groups arise from the low abundance and minimal canting of the HH1 conformer and possibly from the adverse effects of an abundant ΔHT1 conformer. The new findings advance our understanding of the chemistry of the Pt(d(G*pG*)) macrocyclic ring and of the effects of carrier-ligand steric bulk on the properties of the ring.

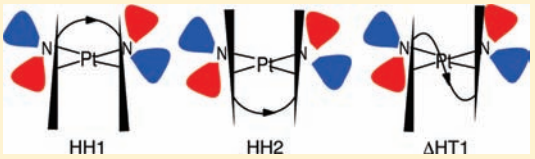

INTRODUCTION

Bifunctional drugs of the type *cis*-PtA_2X_2 [A_2 = one diamine or two amine carrier ligands, X_2 = anionic leaving ligand(s)], including cisplatin (*cis*-Pt$(NH_3)_2Cl_2$) and oxaliplatin, have enjoyed broad clinical usage, now stretching over three decades for cisplatin.[1−9] These and other diverse Pt(II) anticancer compounds target DNA and bind preferentially at the N7 atom of the guanine base (G* = N7-platinated G residue, Figure 1). The bifunctional agents most frequently bind adjacent G residues, creating an intrastrand G*G* cross-link lesion believed to be responsible for activity.[7,8,10−17] A long-recognized consequence of formation of a 17-membered Pt(d(G*pG*)) macrocyclic ring (Figure 2) in the cross-link is the distortion of the G*G* base-pair step, featuring unstacking of the bases and a high degree of canting of one base.[18−20] However, more recently, NMR and X-ray studies of duplex oligomers containing the intrastrand cisplatin lesion[21,22] (and even more recently an oligomer adduct of a rather bulky monofunctional Pt anticancer agent[23,24]) have all revealed a similar and unusual location of the base pair adjacent to the 5′-G* base pair. Thus, the XG* base-pair step is also distorted. These findings have suggested to us that despite the small size of the ammonia ligand, the restraints imposed by the sugar−phosphate backbone result in large interligand interactions of ammonia with the X residue in the XG* base-pair step in DNA with a G*G* intrastrand cross-link formed by cisplatin.[25] The positions of these X, 5′-G*, and 3′-G* residues (and hence the distortions) are modulated by the canting of the bases in the cross-link.

The screening of a large number of bifunctional *cis*-PtA_2X_2 cisplatin analogues with carrier ligands varying in size and properties[26,27] revealed a decrease in activity across the series A = NH_3 > RNH_2 > R_2NH.[6,10,26,28,29] We note that most of the emphasis on explaining the trend has been placed on the role of hydrogen bonding by the carrier-ligand NH groups.[30] However, even when the carrier ligand has no NH groups, some anticancer activity has been detected.[31] Only a few biological studies have been reported on those *cis*-PtA_2X_2 compounds in which the *cis*-A_2 carrier ligand is an *N*,*N*,*N*′,*N*′-tetraalkyldiamine.[29,32] For example, **Me$_4$EN**PtCl_2 (*N*,*N*,*N*′,*N*′-tetramethylethylenediamine; bidentate carrier ligands are designated with boldface type) has been tested

Received: February 7, 2011
Published: April 21, 2011

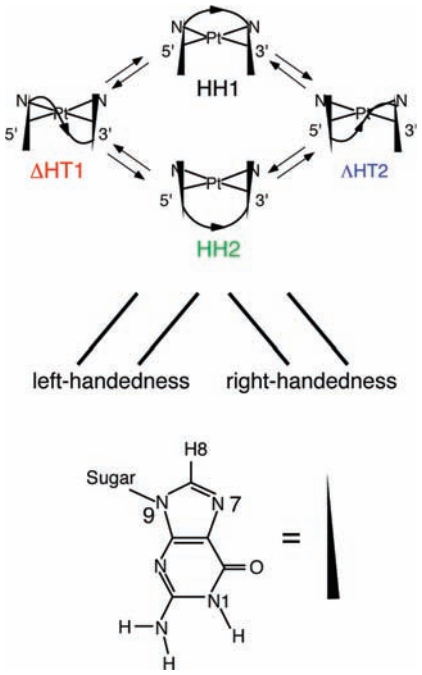

Figure 1. (Top) Four possible conformers of adducts containing the Pt(d(G*pG*)) macrocyclic chelate ring. The G* base (bottom) is depicted as a black triangle with five- and six-membered rings at the tip and base, respectively. The 3′-G* residue has the syn conformation in the ΔHT1 conformer. All other residues are anti. Right (R) and left (L) canting of bases (middle) is shown. Canting direction is independent of the HH or HT base orientation. For simpler models with unlinked bases, the HT chirality is defined as in this figure, but in general, there is only one HH conformer. Conformer designations in this figure and elsewhere are color coded.

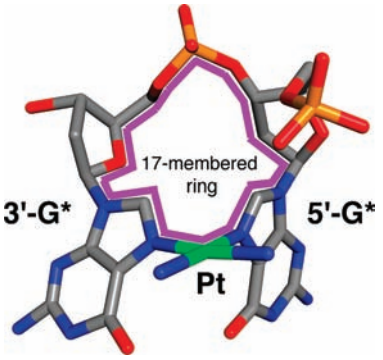

Figure 2. Representative structure of the Pt(G*pG*) cross-link. Pt links adjacent G* residues to form the typical HH1 conformer. The view was chosen to show the anti conformation of the G* residues and the 17-membered chelate ring (outlined in purple) in an HH1 G*G* lesion. [The figure was generated by PyMOL (www.pymol.org) using molecule R1, one of the four *cis*-Pt$(NH_3)_2$(d(pG*pG*)) structures characterized by X-ray crystallography.[18]]

for cytotoxic effects on human ovarian carcinoma cells.[31] Also, bulky N-alkyl groups were found to decrease significantly the cytotoxicity of platinum complexes toward leukemia L1210 cells.[33]

In this work we focus on how high carrier-ligand bulk influences the structure of the Pt(d(G*pG*)) macrocycle (Figure 2) and the number and distribution of the various conformers containing this

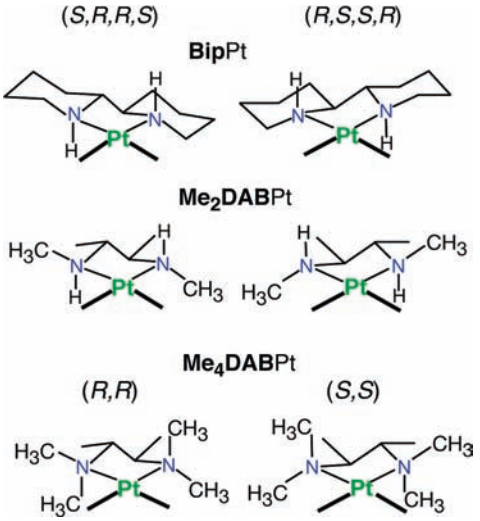

Figure 3. Sketches of the **Bip**Pt and **Me$_2$DAB**Pt moieties with *R,S,S,R* or *S,R,R,S* chirality (stereochemistry defined for the N, C, C, and N ring atoms of the carrier-ligand backbone) and **Me$_4$DAB**Pt moieties with *S,S* or *R,R* chirality (stereochemistry defined for the carbon ring atoms of the carrier-ligand backbone).

ring. The sugar−phosphate backbone in the Pt(d(G*pG*)) macrocycle highly favors the head-to-head (HH) conformation (cf. Figure 1), as compared to *cis*-PtA_2**G**$_2$ adducts, which lack backbone restraints between the bases (boldface **G** = unlinked guanine derivative, cf. Figure 1).[18,34,35] The latter highly favor the head-to-tail (HT) conformers over the HH conformer,[32,36−41] with very few exceptions.[42,43] Interconversions between HH and HT conformations (cf. Figure 1) via rotation about the Pt−**G** N7 bonds in *cis*-PtA_2**G**$_2$ adducts and about the Pt−G* N7 bonds in cross-link adducts are rapid on the NMR time scale.[15,20,32,44−46] Bulky carrier ligands are needed to lower the rotation rate to permit observation of resolved NMR signals of the conformers present in solution.[20,25,36−43,47] In pioneering studies, **Me$_4$EN**Pt**G**$_2$ adducts were shown to exist only as HT conformers in the solid state and in solution.[29,32] Thus, in very early work, the linked *cis*-PtA_2(d(G*pG*)) adducts appeared to be limited to the HH conformation (the carrier ligands were small), and the unlinked adducts conformationally characterized in solution had only the HT conformation (the carrier ligands were large).[20]

Subsequently, employing carrier ligands of intermediate bulk (**Me$_2$DAB** = *N,N*′-dimethyl-2,3-diaminobutane and **Bip** = 2,2′-bipiperidine, Figure 3), we showed that the HH conformer of *cis*-PtA_2**G**$_2$ adducts can exist in solution.[10,15,25,36,37,39−42,44,49] The **Me$_2$DAB**Pt and **Bip**Pt moieties have *S,R,R,S* and *R,S,S,R* enantiomeric C_2-symmetric configurations, in which the chiral centers refer to the N, C, C, and N chelate ring atoms, respectively (Figure 3).

Multiple conformers (Figure 1) were also discovered subsequently for **Bip**Pt(d(G*pG*)) complexes.[44,49] For (*R,S,S,R*)-**Bip**Pt(d(G*pG*)), abundant HH1 and HH2 conformers of comparable stability were found.[44] Compared to the well-known HH1 conformer, the newly discovered conformer (HH2, Figure 1) has the opposite direction of propagation of the phosphodiester backbone with respect to the 5′-G* (with Pt to the rear, the progression from 5′ to 3′ along the backbone is clockwise in HH1 and counterclockwise in HH2). For (*S,R,R,S*)-**Bip**Pt(d(G*pG*)), two conformers were found.[49] One was determined to be

dx.doi.org/10.1021/ic200259s |*Inorg. Chem.* 2011, 50, 4559–4571

HH1, and the other was shown to be the new ΔHT1 conformer (Figure 1), which has the following characteristics: HT bases with the Δ chirality; a clockwise phosphodiester backbone propagation direction; and an *anti*-5′-G* and a *syn*-3′-G*. However, the interesting question of whether high bulk can completely suppress both base canting and formation of an HH conformer, even when a Pt(d(G*pG*)) macrocycle is present in the adduct, remained unanswered.

In order to answer this question, we again chose to use chiral ligands, in this case **Me$_4$DAB** (*N*,*N*,*N*′,*N*′-tetramethyl-2,3-diaminobutane, Figure 3). The coordinated **Me$_4$DAB** ligand has two energetically favored C_2-symmetric geometries, with *S*,*S* or *R*,*R* configurations at the asymmetric C atoms (Figure 3).[30] The chirality allowed us to use NMR methods to establish the absolute conformation of the HT conformers. Our studies on **Me$_4$DAB**Pt**G**$_2$ adducts[30] and those with related chiral *N*,*N*,*N*′,*N*′-tetramethyldiamine ligands[50] indicated that only ΔHT and ΛHT conformers form in observable amounts, consistent with earlier studies on **Me$_4$EN**Pt**G**$_2$ adducts.[29,32,48]

HT conformers can exist in this crowded environment because HT conformers have a favorable (base dipole)−(base dipole) interaction and well-separated, nonclashing **G** O6 atoms. The absence of the HH conformer of **Me$_4$DAB**Pt**G**$_2$ adducts[30] can be attributed to the significant repulsive clashes between the **G** O6 atoms on the cis **G**'s that are likely to occur in an HH conformer. These clashes would be severe because steric interactions of the **Me$_4$DAB** N−Me groups with the **G** bases constrain the bases in positions approximately perpendicular to the coordination plane, thus restricting canting. Also, HH conformers have an unfavorable (base dipole)−(base dipole) repulsion, particularly in **Me$_4$DAB**Pt**G**$_2$ adducts, in which the bases are constrained to be nearly perpendicular to the coordination plane. In this study, we examine **Me$_4$DAB**Pt(d(G*pG*)) adducts by NMR methods and provide extensive analysis of the underlying factors that influence conformer stability and base canting.

EXPERIMENTAL SECTION

Materials. Deoxyguanylyl(3′-5′)deoxyguanosine (d(GpG)) was purchased from Sigma. (*S*,*S*)-**Me$_4$DAB**Pt$(NO_3)_2$ and (*R*,*R*)-**Me$_4$DAB**Pt$(NO_3)_2$ were prepared as described.[30]

Preparation of Platinated d(G*pG*) Adducts. Typically, a ∼1−2 mM sample of d(GpG) was prepared in ∼1 mL of D_2O. The appropriate volume of a $[$**Me$_4$DAB**Pt$(D_2O)_2]^{2+}$ solution (∼2.5 mM) was then added to this solution to give a 1:1 ratio. The reaction mixture (pH ≈ 4, uncorrected) was kept at ∼5 °C until reaction completion. Reactions were monitored by using G* H8 NMR signals until all of the free d(GpG) had been consumed. After the G* H8 signals had indicated complete reaction, the pH was lowered to ∼1.3−1.7. The absence of significant chemical shift changes for the G* H8 signals confirmed Pt−G N7 binding.[51,52]

NMR Spectroscopy. NMR spectra were obtained on a Varian (Unity or Inova) 600 MHz and Bruker Avance II (700 MHz ^{1}H) spectrometer equipped with a cryoprobe, processed with Felix (San Diego, CA) or NMRPIPE,[53] and analyzed with NMRVIEW.[54] The 2D phase-sensitive NOESY and COSY spectra were performed at 5 or 10 °C and pH ≈ 4 (mixing time = 500 ms). The decoupled ^{1}H−^{13}C heteronuclear multiple quantum coherence (HMQC) and heteronuclear multiple bond correlation (HMBC) data were collected at 25 °C. For the HMBC experiment, the $^1J_{CH}$ and $^nJ_{CH}$ coupling values were 175 and 7 Hz, respectively. The ^{31}P NMR spectra were referenced to external trimethyl phosphate. For ^{195}Pt NMR spectroscopy, the (*S*,*S*)-**Me$_4$DAB**Pt(d(G*pG*)) NMR sample was prepared as described above but at ∼10 mM Pt, and data were collected on a Varian Unity 600 MHz instrument operating at 128.6 MHz (Na_2PtCl_6 external reference). Relative percentages of conformers were calculated by using G* H8 or N−Me signals of the **Me$_4$DAB** ligand when the H8 signals overlapped. For temperature dependence experiments, samples were heated in H_2O to avoid C8H to C8D exchange.

RESULTS

Signal Assignments, Determination of Conformation, and General Observations. Signal assignments (Table 1) and conformer determination (Figure 1) for **Me$_4$DAB**Pt(d(G*pG*)) adducts were achieved by a combination of 1D and 2D NMR methods. NOESY, COSY, HMQC, HMBC, ^{31}P NMR, and ^{195}Pt NMR data were used to assess structural features. Briefly, an H8−H8 NOE cross-peak is characteristic of an HH conformer, whereas the absence of such a cross-peak is indicative of an HT conformer.[44,49] For typical *cis*-PtA_2(d(G*pG*)) complexes, HH conformers exhibit H8 and ^{31}P NMR signals more downfield than those of the free d(GpG) dinucleotide,[55−60] whereas HT conformers have more upfield-shifted H8 and ^{31}P NMR signals.[44−46,49] Intraresidue H8−H3′ NOE cross-peaks are characteristically observed for N-sugars but not for S-sugars.[61] Sugar conformations were also deduced from H1′ coupling patterns.[62] Strong H8−H2′/H2″ and weak (or unobservable) H8−H1′ intraresidue NOE cross-peaks are characteristic of anti residues, while strong H8−H1′ intraresidue NOE cross-peaks are typically found for syn residues.[61−63]

The two possible *anti*,*anti*-HH conformers, HH1 or HH2 (Figure 1), which differ primarily in the directions of phosphodiester backbone propagation,[44] exhibit few spectral differences. The HH2 conformer was observed previously for (*R*,*S*,*S*,*R*)-**Bip**Pt(d(G*pG*)), **Me$_2$ppz**Pt(d(G*pG*)), and **5,5′-Me$_2$bipy**Pt(d(G*pG*)).[11,44,46] For the **Bip**Pt(d(G*pG*)) adduct, the HH conformers (each right-handed with one clearly canted base) are easily distinguished by the fact that this canted base resides in the 3′-G* residue in HH1 and in the 5′-G* residue in HH2. When neither residue has a clearly canted base, the presence of 3′-G* H8-sugar NOE cross-peaks for the HH1 conformer and the absence of such cross-peaks for the HH2 conformer permit assignment of the conformers.[44] In general, the appearance of G* H8 signals in pairs downfield for HH conformers and the disappearance of signals of free d(GpG) were used to monitor reactions, normally at 5 °C and pH ≈ 4. Relative to the H8 signals of free d(GpG), the new H8 signals were downfield for the HH conformers and relatively unshifted for the ΔHT1 conformer. Selected figures and tables of NMR data of the adducts not included in the text and tables of NMR data for unplatinated d(GpG) are presented in the Supporting Information.

(*R*,*R*)-Me$_4$DABPt(d(G*pG*)). At ∼6 h after initiation of the reaction of d(GpG) with an (*R*,*R*)-$[$**Me$_4$DAB**Pt$(D_2O)_2]^{2+}$ solution at pH 4, two new pairs of G* H8 signals of equal intensity were present downfield of the free d(GpG) H8 signals. After 1 day, a third pair of G* H8 signals appeared upfield (7.96 and 8.02 ppm) while one pair of downfield signals (8.80 and 8.95 ppm) decreased in intensity. After 4 days, the reaction was complete. Equilibrium was reached in 10 days (final distribution 54% HH1, 38% ΔHT1, 8% HH2). Signals for the three conformers (Figure 4) are assigned below.

In the 2D NOESY spectrum obtained for (*R*,*R*)-**Me$_4$DAB**Pt(d(G*pG*)), an NOE cross-peak was observed between the two

dx.doi.org/10.1021/ic200259s |*Inorg. Chem.* 2011, 50, 4559–4571

Table 1. ^{1}H and ^{31}P NMR Shifts (ppm) and $J_{H1'H2'}/J_{H1'-H2''}$ Values (Hz) for Me_4DABPt(d(G*pG*)) Adducts[a]

conformer (%)	G*	H8	H1′	H2′	H2″	$J_{H1'H2'}/J_{H1'-H2''}$	H3′	H4′	base-sugar[b]	^{31}P
					(*R*,*R*)-**Me$_4$DAB**Pt(d(G*pG*))					
HH1 (54%)	5′	8.57	6.26	2.44	2.81	0/7.3	5.24	4.13	anti	−2.28
	3′	9.29	6.27	2.62	2.42	9.9/4.4	4.72	4.20	anti	
HH2 (8%)	5′	8.95	6.19	3.19	2.80	0/6.5	4.87	4.03	anti	−1.84
	3′	8.80	6.14	2.44	2.70	[c]	4.67		anti	
ΔHT1 (38%)	5′	7.96	6.14	3.17	2.54	0/6.1	3.74	4.10	anti	−4.91
	3′	8.02	6.09	3.24	2.50	3.4/8.6	5.02	4.06	syn	
					(*S*,*S*)-**Me$_4$DAB**Pt(d(G*pG*))					
HH1 (34%)	5′	8.65	6.26	2.45	2.82	0/7.5	5.25	4.14	anti	−2.27
	3′	9.27	6.25	2.60	2.40	9.1/5.0	4.71	4.20	anti	
ΔHT1 (66%)	5′	7.96	6.13	3.23	2.54	0/6.3	3.74	4.10	anti	−4.93
	3′	8.01	6.08	3.22	2.50	3.5/8.6	5.02	4.05	syn	

[a] 2D experiments conducted at 5 °C, pH ≈ 4.0 (100% D_2O). [b] Anti/syn conformational assignment based on the relative strength of NOE cross-peaks between H8 resonances and H1′ or H2′/H2″ signals. [c] Not determined.

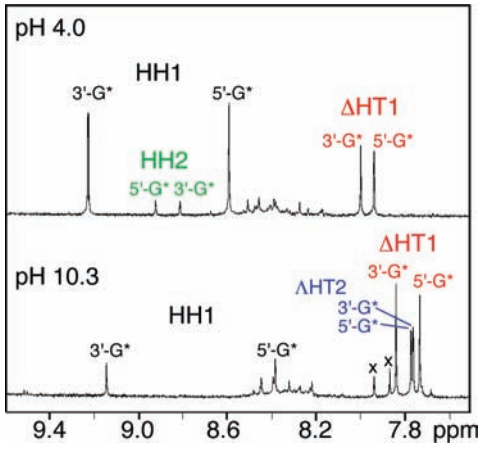

Figure 4. G* H8 region of the 1D ^{1}H NMR spectra of equilibrium mixtures of (*R*,*R*)-**Me$_4$DAB**Pt(d(G*pG*)) conformers at room temperature and the indicated pH values (in 100% D_2O). Signals marked with × indicate an uncharacterized minor species.

H8 signals of the most abundant conformer (Figure 5). As described above, an H8−H8 cross-peak is characteristic of an HH conformer. The more upfield H8 signal (8.57 ppm) showed a strong NOE cross-peak to a signal at 2.44 ppm and a weaker cross-peak to a resonance at 2.81 ppm. NOE cross-peaks were observed between the signals at 2.44 and 2.81 ppm, the latter showing a cross-peak to a signal at 6.26 ppm. Another NOE cross-peak was also observed between signals at 6.26 and 4.13 ppm. The H8 signal at 8.57 ppm also showed a strong NOE cross-peak to a signal at 5.24 ppm (Figure 5). These observations, along with COSY data, allowed assignment of the signals to H1′, H2′, H2″, H3′, and H4′ sugar protons (Table 1). The strong H8−H3′ NOE cross-peak indicates an N-sugar pucker,[61,62] consistent with a 5′-G*.[19,44,56] The presence of H8−H2′ and H8−H2″ NOE cross-peak signals and the very weak nature of the H8−H1′ cross-peak are both consistent with the 5′-G* residue having an anti conformation.

The more downfield H8 signal (9.29 ppm), which belongs to the 3′-G* residue, showed NOE cross-peaks to signals at 2.42 and 2.62 ppm, the latter cross-peak being the stronger of the two. NOE cross-peaks connected the 2.42 and 2.62 ppm signals, which also had NOE cross-peaks to a signal at 6.27 ppm. The 2.42−6.27 ppm NOE cross-peak was strong, while the 2.62−6.27 ppm cross-peak was comparatively weak. An additional NOE was observed between signals at 6.27 and 4.20 ppm. The latter had a cross-peak with a signal at 4.72 ppm. These observations, along with COSY data, allowed assignment of the 3′-G* H1′, H2′, H2″, H3′ and H4′ signals (Table 1). The intranucleotide H8−H2′/H2″ NOE cross-peaks and the very weak H8−H1′ NOE cross-peak suggest an anti 3′-G* conformation.[61,63,64] These spectral features in an HH conformer, especially the presence of many medium to strong NOE cross-peaks from the H8 signals to the sugar signals, are consistent with an HH1 conformer (Figure 1).

The second most abundant conformer had spectral features that are very different from those of the most abundant HH1 conformer. No NOE cross-peak was observed between the relatively upfield H8 signals of this conformer (Figure 5). The more upfield H8 signal (7.96 ppm) showed NOE cross-peaks to signals at 6.14, 3.74, and 3.17 ppm. Strong NOE's were observed between the signals at 6.14 ppm and signals at 3.17 and 2.54 ppm (Figure 5); however, a weak NOE was also detectable between the signals at 6.14 and 4.10 ppm. These cross-peaks allowed assignment of signals to H1′, H2′, H2″, H3′, and H4′ protons (Table 1). These assignments were all confirmed by COSY data. The weak H8−H1′ and strong H8−H2′ NOE cross-peaks suggest an anti G* residue.[61,63,64] The presence of an H8−H3′ cross-peak is consistent with an N-sugar pucker;[62] these signals are assigned to the 5′-G* residue (Table 1).

The more downfield H8 signal (8.02 ppm), belonging to the 3′-G* residue of the second most abundant conformer, showed a strong NOE cross-peak to a signal at 6.09 ppm (Figure 5). This signal at 6.09 ppm showed NOE and COSY cross-peaks to two signals at 2.50 and 3.24 ppm; the 6.09−2.50 ppm NOE cross-peak was stronger than the 6.09−3.24 ppm NOE cross-peak. An NOE cross-peak between the signal at 6.09 ppm and a signal at 4.06 ppm was also observed. The signal at 4.06 ppm showed an NOE cross-peak to the signal at 2.50 ppm. An additional NOE was observed between the signals at 3.24 and at 5.02 ppm. These observations allowed assignment of the 3′-G* H1′, H2′, H2″, H3′, and H4′ signals (Table 1). The strong H8−H1′ NOE cross-peak indicates that this 3′-G* residue has a syn conformation.[61]

dx.doi.org/10.1021/ic200259s |*Inorg. Chem.* 2011, 50, 4559–4571

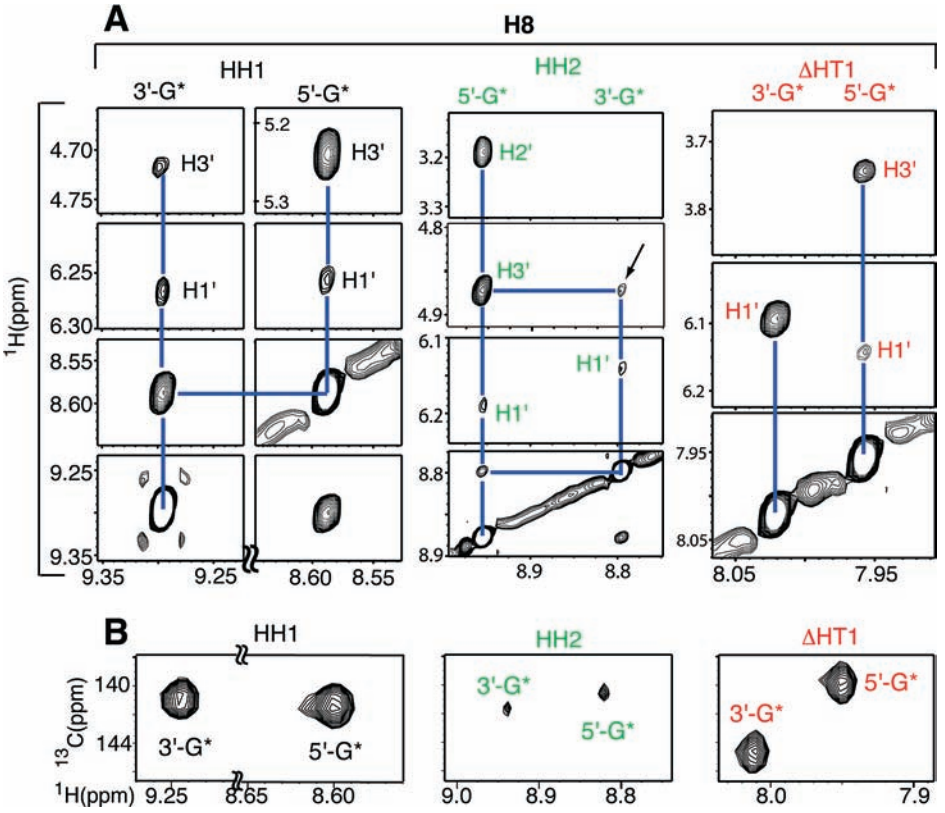

Figure 5. Selected regions of the 2D NOESY (top) and HMQC (bottom) spectra obtained for (*R*,*R*)-**Me$_4$DAB**Pt(d(G*pG*)) at pH 4.0 (in 100% D_2O).

Spectral features observed for this conformer are consistent with the ΔHT1 conformation (Figure 1).[11,46,49]

For the third and least abundant conformer, the NOESY data showed an H8−H8 cross-peak (Figure 5). The H8 signal at 8.95 ppm gave weak NOE cross-peaks to signals at 6.19 and 2.80 ppm and strong NOE cross-peaks to signals at 4.87 and 3.19 ppm. The 3.19 and 2.80 ppm signals had NOE cross-peaks to each other and to the signal at 6.19 ppm. A weak NOE cross-peak was observed between signals at 4.03 and 4.87 ppm. From these observations and the intensity pattern in the NOESY and COSY data, we assigned these signals to H1′, H2′, H2″, H3′, and H4′ of the 5′-G* residue because the H8−H3′ NOE cross-peak indicates an N-sugar pucker.[21,44,46,49,59,60,65] This residue is anti because a strong H8−H2′ NOE cross-peak was observed, while the H8−H1′ NOE cross-peak was very weak.[61,63,64]

The other H8 signal (8.80 ppm) for the third conformer must be that of the 3′-G* residue. This signal showed two very weak signals at 6.14 and 4.87 ppm. Strikingly, the latter peak is assigned to the 5′-G* H3′ signal. This is the first evidence of an intramolecular internucleotide NOE between the G* H8 and a sugar proton of an adjacent G* in a dinucleotide cross-link. Another NOE was observed between this H8 signal and a signal at 2.44 ppm, which had an NOE cross-peak to a signal at 2.70 ppm. The signals at 2.44 and 2.70 ppm both had NOE's to a signal at 4.67 ppm. This NOE pattern allowed assignment of the 3′-G* H1′, H2′, H2″, and H3′ signals (Table 1). Spectral features of this third conformer, such as the weakness of the 3′-G* H8 to sugar NOE cross-peaks, are consistent with those expected for the HH2 conformer (Figure 1). Furthermore, the 3′-G* H8 to 5′-G* H3′ cross-peak is consistent with models of the HH2 conformer but not with models of the HH1 conformer.[44,46]

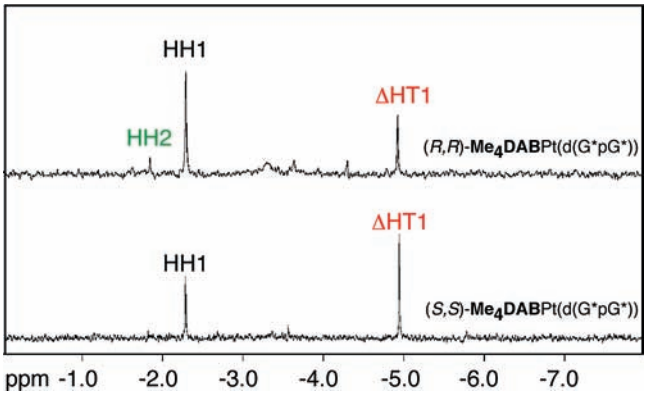

Figure 6. ^{31}P NMR spectra of **Me$_4$DAB**Pt(d(G*pG*)) adducts at pH 4.0 (25 °C, 100% D_2O). Unlabeled minor signals are likely to be impurities.

The similarity of the three ^{31}P NMR resonances clearly observed at −2.28, −1.84, and −4.91 ppm (Figure 6, Table 1) to chemical shifts observed for *cis*-PtA_2(d(G*pG*)) adducts confirmed the ^{1}H NMR assignments.[11,44,46,49] The relative intensities of these three signals are consistent with their assignment to the HH1, HH2, and ΔHT1 conformers, respectively.

Because a distorted geometry can produce large differences in G* C8 shifts[66] and because sugar pucker can be assessed by using ^{13}C NMR shifts of C3′ signals, we obtained ^{1}H−^{13}C HMQC NMR data (Table 2). The presence of three conformers (HH1, HH2, and ΔHT1) for the (*R*,*R*)-**Me$_4$DAB**Pt(d(G*pG*)) adduct afforded a good opportunity to correlate structural features with ^{13}C NMR data and to compare the results with ^{13}C NMR data for (*S*,*S*)-**Me$_4$DAB**Pt(d(G*pG*)) (see below).

dx.doi.org/10.1021/ic200259s |*Inorg. Chem.* 2011, 50, 4559–4571

Table 2. ^{13}C NMR Shifts (ppm) of Me_4DABPt(d(G*pG*)) Adducts (25 °C, pH ≈ 4, 100% D_2O)

	conformer		C8	C4	C5	C1′	C2′	C3′	C4′
(*R*,*R*)-**Me$_4$DAB**Pt(d(G*pG*))	HH1	5′-G*	141.7			84.5	42.2	73.5	87.3
		3′-G*	141.3			85.0	42.8	73.6	88.8
	HH2	5′-G*	141.7			90.0	40.0	72.1	
		3′-G*	140.6			89.2	42.3	73.9	
	ΔHT1	5′-G*	140.2			90.3	40.7	72.8	88.2
		3′-G*	145.1			89.4	39.6	73.5	88.7
(*S*,*S*)-**Me$_4$DAB**Pt(d(G*pG*))	HH1	5′-G*	141.7	153.8	116.1	84.4	42.3	73.4	87.3
		3′-G*	141.5	154.1	116.7	85.0	42.9	73.6	88.8
	ΔHT1	5′-G*	140.2	153.3	117.8	90.3	40.8	72.8	88.3
		3′-G*	144.9	154.2	117.2	89.3	39.6	73.5	88.7

Typically, **G** C8 signals shift from ∼140.5 to ∼141.5 ppm on platination of guanine derivatives at N7.[59] The G* C8 chemical shifts for the HH1 and HH2 conformers of (*R*,*R*)-**Me$_4$DAB**Pt(d(G*pG*)) are almost identical (∼141.5 ppm, Figure 5 and Table 2). Interestingly, these C8 shifts are also similar to those observed for the HT conformers of **Me$_4$DAB**Pt**G**$_2$[30] and Pt−oligo adducts.[21,59,66] For the ΔHT1 conformer, the 5′-G* C8 chemical shift is slightly upfield to those of the HH conformers. However, the 3′-G* C8 signal for the ΔHT1 conformer is shifted distinctly downfield (145.1 ppm). These results suggest an unusual positioning of the 3′-G* base and possibly the 5′-G* base of the ΔHT1 conformer.

For (*R*,*R*)-**Me$_4$DAB**Pt(d(G*pG*)), the 5′- and 3′-G* C3′ signals for the HH1 and ΔHT1 conformers were detected at ∼73 ppm (Table 2 and Supporting Information). The upfield 3′-G* C3′ shifts observed for the HH1 and ΔHT1 conformers are typical of those for 3′-terminal residues with an S-pucker.[21,59] In our previous studies on cisplatin DNA adducts containing G*pG* intrastrand cross-links,[21,59,66] the C3′ sugar signal of the 5′-G* residue was found to have a significant upfield shift (∼72 vs 79 ppm for an unplatinated G residue, Supporting Information) that was related to the N-sugar pucker for the 5′-G* sugar (determined by NOESY and COSY data). The C3′ upfield shift of the 5′-G* residues of the HH1 and ΔHT1 conformers is thus characteristic of an N sugar. The C1′ shifts for both G* residues of the HH1 conformer were similar to those of the unplatinated G (∼85 ppm, Table 2 and Supporting Information), but the ΔHT1 and HH2 C1′ signals exhibited very downfield shifts (∼90 ppm). C8 and C1′ signals are known to be more downfield in syn G* than in anti G* residues.[66,67] Compared to the HH1 conformer and to previous observations,[59] the ΔHT1 and HH2 conformers have a few somewhat different ^{13}C NMR shifts consistent with some unusual, perhaps strained structural components. Similar data are not available for adducts with other carrier ligands. Nevertheless, because the ^{1}H and ^{31}P NMR shifts are similar to those found for adducts with other carrier ligands,[11,44,46,49] these features are undoubtedly not restricted to **Me$_4$DAB**Pt(d(G*pG*)) adducts. This is our first ^{13}C NMR study on HT and HH2 conformers for a Pt(d(G*pG*)) cross-link adduct.

For the abundant HH1 and ΔHT1 conformers, the ^{13}C NMR signals of the eight **Me$_4$DAB** N−Me groups could be assigned by ^{1}H−^{13}C HMQC data (Supporting Information), which revealed a characteristic pattern. For the HH1 conformer, ^{13}C NMR shifts for the two equatorial N−Me groups were 53.6 (H8 side of 5′-G*) and 53.1 (O6 side of 3′-G*) ppm. For the two axial N−Me groups, ^{13}C NMR shifts were 47.6 (O6 side of 5′-G*) and 46.3 (H8 side of 3′-G*) ppm. For the ΔHT1 conformer, the axial N−Me signals were 46.6 (O6 side of 3′-G*) and 46.9 (O6 side of 5′-G*) ppm, whereas the equatorial N−Me signals were both at 54.1 ppm. The distinct pattern of the axial and equatorial N−Me ^{13}C signals was also observed for the **Me$_4$DAB**Pt**G**$_2$ adducts.[30] This significant dependence of the ^{13}C NMR shifts of the N−Me groups on the axial/equatorial nature of these groups cannot be attributed to guanine base anisotropic effects because the ^{1}H NMR shifts of the N−Me groups do not vary in a correlated way with the ^{13}C NMR shifts of the corresponding N−Me groups, and the ^{1}H NMR shifts, which are expected to be more sensitive to the anisotropic effect, vary by only ∼0.3 ppm. This dependence of the ^{13}C NMR shifts is probably a result of strain caused by the different relationship of the C−Me group to the N−Me groups or a result of ligand or Pt(II) inductive effects differing somewhat for axial vs equatorial N−Me groups.[30,68]

To understand the intrinsic factors that contribute to the stability of HH vs HT conformers, we examined the effect of pH on conformer distribution of the (*R*,*R*)-**Me$_4$DAB**Pt(d(G*pG*)) adduct as a function of time after increasing the pH from 4.0 to 10.3 (initial and final spectra are shown in Figure 4). In the first spectrum recorded (∼20 min) after the pH was increased, all the H8 signals were shifted upfield by 0.1−0.2 ppm. The HH2 signals were approximately one-half as intense as in the spectrum recorded at pH 4.0. This spectrum contained two very small signals at 7.75 and 7.76 ppm. ROESY, COSY, and ^{1}H−^{13}C HMQC data collected at pH 10.3 (discussed in Supporting Information) suggest that this new conformer is the ΛHT2 conformer and that it can exist for this adduct only at high pH. After 1 h at pH 10.3, the HH2 H8 signals were barely visible and the two H8 signals of the ΛHT2 conformer had increased in intensity. Within 2 h, the HH2 signals disappeared, while the signals of the ΛHT2 conformer continued to increase in intensity. After 8 h, another two new H8 signals (at 7.87 and 7.94 ppm) were observed; the low intensity made it impossible to characterize this fifth species. After 2 days, changes in signal intensities ceased (Figure 4), indicating that equilibrium had been reached. The final distribution was 14% HH1, 28% ΛHT2, and 58% ΔHT1. Three ^{31}P NMR resonances for (*R*,*R*)-**Me$_4$DAB**Pt(d(G*pG*)) at pH 10.3 observed after equilibrium had been reached (Supporting Information) were assigned from their relative intensity and from the chemical shift similarities to those observed at pH 4.0. ^{31}P NMR signals at −2.26 and −4.93 ppm are assigned to the HH1 and ΔHT1 conformers, respectively. A third ^{31}P NMR signal at −4.2 ppm is most likely that of the ΛHT2 conformer.

To confirm our conclusion that the new high-pH species is a conformer of (*R*,*R*)-**Me$_4$DAB**Pt(d(G*pG*)), we assessed whether

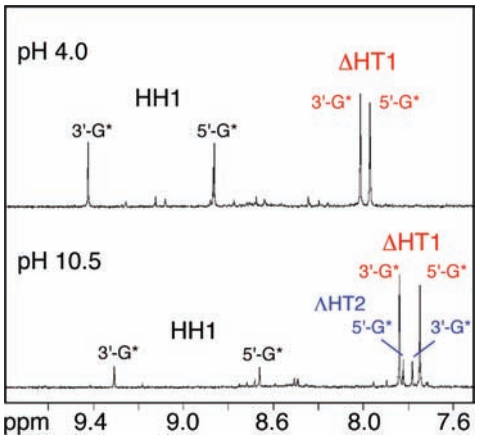

Figure 7. G* H8 region of the 1D ^{1}H NMR spectra of equilibrium mixtures of (*S,S*)-**Me$_4$DAB**Pt(d(G*pG*)) conformers at room temperature and the indicated pH values (in 100% D_2O).

the pH-induced changes in distribution are reversible. The pH was dropped to 4.0, and changes in distribution were monitored with time. The H8 signals of the ΛHT2 conformer decreased in intensity shortly after the pH was dropped (~20 min) and were no longer observed after 2 h at pH 4.0. Two days after the pH was dropped, the distribution was similar to the pH 4, 25 °C distribution (54% HH1, 38% ΔHT1, and 8% HH2) observed before the pH was increased. Thus, the effect of high pH is reversible. To examine the conformer distribution at high temperature, ^{1}H NMR spectra were collected at 60 °C and pH 4.0. The H8 signals of the HH1, HH2, and ΔHT1 conformers did not shift significantly between 25 and 60 °C. After 3 days at 60 °C, the distribution changed to 33% HH1, < 1% HH2, and 67% ΔHT1. Compared to the pH 4.0, 25 °C distribution just given, these results indicate that the HH1 conformer is relatively less stable and that ΔHT1 is relatively more stable both at high pH (10.3) and at high temperature (60 °C). Nevertheless, the HH1 conformer of the (*R,R*)-**Me$_4$DAB**Pt(d(G*pG*)) adduct exists at a significant level under all conditions investigated.

(*S,S*)-Me$_4$DABPt(d(G*pG*)). Throughout the course of the reaction forming the (*S,S*)-**Me$_4$DAB**Pt(d(G*pG*)) adduct, the newly observed H8 signals differed in number and relative intensity from those described above for the reaction forming the (*R,R*)-**Me$_4$DAB**Pt(d(G*pG*)) adduct. Only two new pairs of G* H8 signals were clearly observed 1 day after initiation of the reaction (pH 4.0), indicating formation of only two new conformers. The reaction was complete in 5 days, with a final distribution of 34% HH1 and 66% ΔHT1 determined by using H8 signal intensities (Figure 7). [Assignment of the two conformers of (*S,S*)-**Me$_4$DAB**Pt(d(G*pG*)) was achieved by analyzing a combination of 1D (^{1}H and ^{31}P) and 2D (NOESY, COSY, ^{1}H−^{13}C HMQC, and ^{1}H−^{13}C HMBC) NMR data.] The ^{1}H NMR chemical shifts for these two conformers are very similar to those observed for the corresponding conformers of the (*R,R*)-**Me$_4$DAB**Pt(d(G*pG*)) adduct (Table 1).

In the ^{1}H−^{13}C HMQC spectrum obtained for (*S,S*)-**Me$_4$DAB**Pt(d(G*pG*)), the 5′-G* and 3′-G* C8 signals of the HH1 conformer were detected at ~141.6 ppm (Figure 8 and Table 2). As observed for the (*R,R*)-**Me$_4$DAB**Pt(d(G*pG*)) adduct in comparing the HH1 and ΔHT1 conformers, the 5′-G* C8 signal for the ΔHT1 conformer had a slightly upfield shift (140.2 ppm) while the 3′-G* C8 signal was more downfield (144.9 ppm). In addition, the G* C1′ shifts for the HH1 and

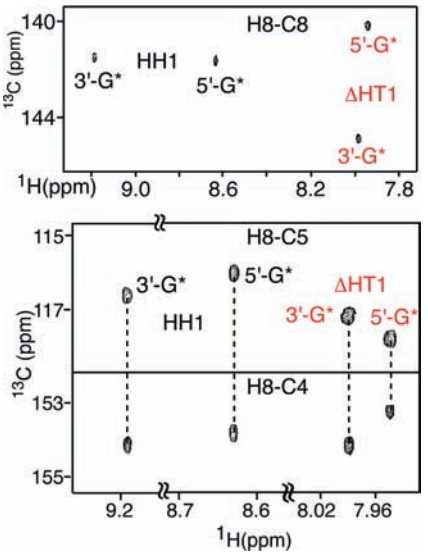

Figure 8. Selected regions of 2D ^{1}H−^{13}C HMQC (top) and HMBC (bottom) spectra obtained for (*S,S*)-**Me$_4$DAB**Pt(d(G*pG*)) at pH ≈ 4 and 25 °C (in 100% D_2O).

ΔHT1 conformers were also very similar to the corresponding signals in the (*R,R*)-**Me$_4$DAB**Pt(d(G*pG*)) adduct (Table 2). These results indicate that the ΔHT1 conformer has almost exactly the same structural features in both adducts. The shifts of the 5′- and 3′-G* C3′ signals for the (*S,S*)-**Me$_4$DAB**Pt(d(G*pG*)) HH1 and ΔHT1 conformers are all almost identical to those observed for these conformers of the (*R,R*)-**Me$_4$DAB**Pt(d(G*pG*)) adduct (Table 2), confirming that the sugar moieties of the 5′-G* residues of the HH1 and ΔHT1 conformers have an N-pucker.

In the ^{1}H−^{13}C HMBC spectrum (Figure 8), the HH1 5′-G* H8 signal showed cross-peaks to ^{13}C signals at 153.8 and 116.1 ppm, whereas the 3′-G* H8 signal was coupled to ^{13}C signals at 154.1 and 116.7 ppm. On the basis of previous observations,[59] these ^{13}C signals were assigned to C4 and C5, respectively. For the ΔHT1 conformer, the 5′-G* C4 and C5 ^{13}C NMR signals were observed at 153.3 and 117.8 ppm, whereas those of the 3′-G* residue were assigned at 154.2 and 117.2 ppm, respectively. As discussed above for the (*R,R*)-**Me$_4$DAB**Pt(d(G*pG*)) adduct, these results suggest that the sugar backbone of the ΔHT1 conformer possesses some unique structural features, which may also exist for previously studied *cis*-PtA_2(d(G*pG*)) adducts.[11,46,49] In addition, the very similar ^{13}C NMR shifts for the HH1 and ΔHT1 conformers for both (*R,R*)- and (*S,S*)-**Me$_4$DAB**Pt(d(G*pG*)) adducts indicate that the chirality of the carrier ligand does not appear to have any effect on the structures of conformers.

The ^{13}C NMR signals of the eight N−Me groups of the (*S,S*)-**Me$_4$DAB**Pt(d(G*pG*)) conformers were assigned by the ^{1}H−^{13}C HMQC method (Supporting Information). The ^{1}H and ^{13}C NMR shifts for the N−Me groups are very similar to those observed for the HT conformers of **Me$_4$DAB**Pt**G$_2$**[30] and for the conformers of (*R,R*)-**Me$_4$DAB**Pt(d(G*pG*)) described above.

To examine whether the combination of a bulky **Me$_4$DAB** carrier ligand and bound, linked guanines causes any distortion in the Pt plane, ^{195}Pt NMR shifts were obtained for (*S,S*)-**Me$_4$DAB**Pt(d(G*pG*)) and compared to those for other compounds. ^{195}Pt NMR signal shifts are sensitive parameters that have often been used to identify the number, type, and geometrical arrangement of the coordinated ligands.[69−71] The ^{195}Pt NMR signals

dx.doi.org/10.1021/ic200259s |*Inorg. Chem.* 2011, 50, 4559–4571

for the HT conformers of [*rac*-**Me$_4$DAB**Pt(9-EtG)$_2$]$^{2+}$ overlap at −2492 ppm.[30] This value is very similar to those observed for the **Me$_2$ppz**Pt(5′-GMP)$_2$ HT conformers (**Me$_2$ppz**, *N*,*N*′-dimethylpiperazine).[43] For (*S*,*S*)-**Me$_4$DAB**Pt(d(G*pG*)), two partially overlapping ^{195}Pt NMR signals were observed at −2461 and −2443 ppm (data not shown). On the basis of their relative intensities, these signals were assigned to the HH1 and ΔHT1 conformers, respectively. Thus, although the ΔHT1 conformer appears to be relatively distorted, the Pt coordination sphere does not appear to be distorted. As mentioned, the ^{195}Pt NMR shifts are very sensitive, and even a change from A_2 = $(NH_3)_2$ to A_2 = ethylenediamine causes a change of more than 200 ppm in the ^{195}Pt NMR shift.[70] Thus, the change from **Me$_4$DAB**Pt**G$_2$** to **Me$_4$DAB**Pt(d(G*pG*)) does not seem to induce large changes in the Pt coordination environment.

To assess the underlying factors that contribute to the stability of conformers, we studied the effect of pH on conformer distribution for the (*S*,*S*)-**Me$_4$DAB**Pt(d(G*pG*)) adduct. When the pH was raised from 4.0 to 10.3 and the sample left at this pH for 3 days, a final distribution of 12% HH1 and 88% ΔHT1 was determined by ^{1}H NMR spectroscopy (Figure 7), marking the highest amount of ΔHT1 conformer ever obtained for a *cis*-PtA_2(d(G*pG*)) adduct. As found for (*R*,*R*)-**Me$_4$DAB**Pt(d(G*pG*)), the ^{1}H and ^{31}P NMR spectra for (*S*,*S*)-**Me$_4$DAB**Pt(d(G*pG*)) contained signals for the ΛHT2 conformer that exist only at high pH. All ^{1}H and ^{31}P NMR signals at pH 10.3 obtained after equilibration have shifts nearly identical to those assigned to the HH1, ΔHT1, and ΛHT2 conformers of the (*R*,*R*)-**Me$_4$DAB**Pt(d(G*pG*)) adduct (Supporting Information).

After the pH was lowered to 4.0 at 23 °C, the distribution slowly changed from 12% HH1 and 88% ΔHT1 toward the previous low-pH equilibrium value, 34% HH1 and 66% ΔHT1. Furthermore, as observed for (*R*,*R*)-**Me$_4$DAB**Pt(d(G*pG*)), the HH1 conformer remained present at pH 4.0 when the temperature was increased to 60 °C. The distribution changed to 25% HH1 and 75% ΔHT1 after 3 days at 60 °C. The findings for the (*S*,*S*)-**Me$_4$DAB**Pt(d(G*pG*)) adduct reveal many similarities to those for the (*R*,*R*)-**Me$_4$DAB**Pt(d(G*pG*)) adduct in that both the HH1 and the ΔHT1 conformers are present under all conditions and that the Pt(d(G*pG*)) macrocylic rings for corresponding conformers have almost identical structural features. The main difference between the two **Me$_4$DAB**Pt(d(G*pG*)) adducts is found in the relative abundance of conformers. Most notably, the HH2 conformer is clearly present only in the (*R*,*R*)-**Me$_4$DAB**Pt(d(G*pG*)) adduct.

DISCUSSION

Compared to cisplatin, analogues with NH groups in the carrier ligand replaced by bulky N-alkyl groups are more toxic and less active. In this study, we sought to examine the molecular origins for the biological effects of steric bulk through a thorough analysis of two representative chiral **Me$_4$DAB**Pt(d(G*pG*)) adducts. As expected, from our studies of **Me$_4$DAB**Pt**G$_2$** adducts, the presence of N−Me alkyl groups that impede dynamic motion enhances the utility of NMR methods for identifying and characterizing conformers of the Pt(d(G*pG*)) macrocyclic ring.[30] By using relevant X-ray structural data available for HT conformers of adducts with **G** = 5′-GMP[72] as well as for **Me$_4$EN**Pt**G$_2$** structures,[29] we can estimate N7−Pt−N−C(Me) torsion angles of ∼70−80° for quasi-axial N−Me groups and of 39−48° for quasi-equatorial N−Me groups for bidentate carrier ligands with puckered N−C−C−N−Pt chelate rings. Thus, the relevant steric bulk of **Me$_4$DAB** resides in one quasi-axial and one quasi-equatorial alkyl group on each end of the ligand, and these groups project both above and below the coordination plane.

Although it is not our purpose here to assess the literature X-ray data in detail, suffice it to say that in general the closest approaches of the relevant **G** base atoms (H8, O6, C5, and C6) to the N−Me groups occur for the quasi-equatorial N−Me group. Although the internuclear nonbonded distances are shorter by only 0.1−0.2 Å, these results suggest that the quasi-equatorial N−Me group projects in the direction of the **G** base somewhat more than does the quasi-axial N−Me group.[72] For H8, there is no question that the interaction with the N−Me group is repulsive. For the **G** six-membered ring atoms, especially O6, there is an attractive component between the partially negatively charged O6 and the partially positively charged N−Me protons.

For **Me$_2$DAB** and **Bip** adducts, the carrier-ligand bulk on each end of the ligand resides in just one quasi-equatorial alkyl group on each side of the coordination plane (Figure 3).[25,36,37,39−42,44,49] For **Me$_2$ppz** adducts the relevant carrier-ligand bulk on each end of the ligand resides in just one N−Me group in the coordination plane.[43,46,47,73] The **Me$_2$ppz** carrier ligand is achiral and lacks NH groups. Three conformers coexist in **Me$_2$ppz**Pt(d(G*pG*)) (HH1, HH2, and ΔHT1)[46] in substantial abundance and two each in (*R*,*S*,*S*,*R*)-**Bip**Pt(d(G*pG*)) (HH1, HH2) and (*S*,*R*,*R*,*S*)-**Bip**Pt(d(G*pG*))[49] (HH1 and ΔHT1); however, in the unlinked *cis*-PtA_2**G$_2$** adducts, all three conformers (HH, ΛHT, and ΔHT) usually exist.[36,37,39−43,47] As mentioned, **Me$_4$DAB**Pt**G$_2$** and earlier related adducts do not conform to the typical *cis*-PtA_2**G$_2$** adduct pattern;[30,32] **Me$_4$DAB**Pt**G$_2$** adducts do not form the HH conformer but form only the two HT conformers. Thus, it was not clear whether one should reasonably expect to observe only HT conformers of **Me$_4$DAB**Pt(d(G*pG*)) adducts.

For adducts having carrier ligands inducing slow conformer interchange, the *cis*-PtA_2(d(G*pG*)) cross-link moiety generally favors the HH conformers more than in *cis*-PtA_2**G$_2$** analogues with unlinked **G**'s.[11,44,46,49] For (*R*,*R*)-**Me$_4$DAB**Pt(d(G*pG*)), the G* H8, O6, C5, and C6 atoms of each base can approach an N−Me group of the **Me$_4$DAB** and possibly clash with the N−Me group regardless of conformation. Nevertheless, at least two conformers (HH1 and ΔHT1) in characterizable abundance were observed for both adducts studied here. A third conformer, HH2, was also observed for (*R*,*R*)-**Me$_4$DAB**Pt(d(G*pG*)). Thus, this sterically crowded carrier ligand does not seriously limit the number of conformers formed in comparison to other adducts with less bulky ligands.[44,49] Indeed, the presence of three reasonably abundant conformers at equilibrium was previously observed only in the case of the least sterically hindering carrier ligands.[11,46,73] Furthermore, despite the bulk of the carrier ligand, we also have evidence that a fourth conformer, ΛHT2, of the (*R*,*R*)-**Me$_4$DAB**Pt(d(G*pG*)) adduct exists at high pH.

These rather remarkable findings for **Me$_4$DAB**Pt(d(G*pG*)) adducts have provided some understanding of effects of carrier-ligand bulk. Below we shall discuss the effect of the **Me$_4$DAB** carrier ligand on the structural features, base canting, NMR properties, and distribution and stability of the **Me$_4$DAB**Pt(d(G*pG*)) conformers.

Structural Features of Conformers. It is striking that the corresponding conformers in the **Me$_4$DAB**Pt(d(G*pG*)) adducts, regardless of the carrier-ligand chirality, have almost identical ^{1}H, ^{13}C, and ^{31}P NMR shifts (Table 1). Thus, the chirality of the **Me$_4$DAB** ligand has no influence on the structure of the

Pt(d(G*pG*)) ring of the HH1 and ΔHT1 conformers, and the canting in the conformers (see below) is also not influenced by the **Me$_4$DAB** chirality. As noted in past work, in which the conformers observed had many spectral features that are similar,[44,46,49] the backbone appears to be insensitive to the properties of the carrier ligands. This conclusion can now be broadened to include the **Me$_4$DAB**Pt(d(G*pG*)) adducts and to include support from ^{13}C NMR data. The 5′-G* residue of the HH1 and ΔHT1 conformers for both **Me$_4$DAB**Pt(d(G*pG*)) adducts was found to adopt the N-sugar pucker. Indeed, the N-pucker for the 5′-G* residue is universal in such cross-links.[21,25,44,46,49,59,73] Likewise, the 3′-G* sugar of the HH and HT conformers of **Me$_4$DAB**Pt(d(G*pG*)) adducts has features similar to those of the **Bip**Pt(d(G*pG*)) and **Me$_2$ppz**Pt(d(G*pG*)) analogues.[25,44−46,49,73] For these adducts, the 3′-G* residue of the HH1 and HH2 conformers retains the S sugar conformation favored by the free nucleic acid derivative. The sugar moiety of the 3′-G* residue of the ΔHT1 conformer for **Me$_4$DAB**Pt(d(G*pG*)) adducts has appreciable N-character, consistent with our findings for the **Bip**Pt(d(G*pG*)) and **Me$_2$ppz**Pt(d(G*pG*)) complexes.[46,49] Thus, we conclude that the favored sugar pucker of the 5′-G* and 3′-G* residues is independent of the carrier ligand (**Bip**, **Me$_2$ppz**, **Me$_4$DAB**), even when that ligand is as bulky as **Me$_4$DAB**. This N-pucker feature of the 5′-G* sugar is also observed for cisplatin adducts.[20,59,60,65]

The ΔHT1 conformer in both **Me$_4$DAB**Pt(d(G*pG*)) adducts has a very upfield-shifted ^{31}P NMR signal, consistent with our previous findings.[11,25,46,49] Likewise, the ^{1}H NMR shifts and couplings of the sugar residue are in good agreement, suggesting again that adducts have similar structures, at least in the backbone region, regardless of the nature of the carrier ligand.

^{13}C NMR data proved very useful in identifying the structural features of conformers. For (*S*,*S*)-**Me$_4$DAB**Pt(d(G*pG*)), the similarity of the G* C8 ^{13}C NMR shifts of the HH1 conformer to those observed for this conformer in adducts studied previously[59,66] indicates that the C8 shifts of the HH1 conformer are not dependent on the carrier-ligand bulk. In contrast, the G* C8 ^{13}C NMR shifts of the ΔHT1 conformer (Table 2) were significantly different from most previously reported shifts. C8 and C1′ signals are known to be more downfield in syn G* than in anti G* residues.[66,67] This is our first ^{13}C NMR study on multiconformer *cis*-PtA$_2$(d(G*pG*)) cross-link adducts. Our finding that the C8 and C1′ signals of the 3′-G* residue are consistent with the syn conformation for this residue establishes a potential new fingerprinting method for characterizing the ΔHT1 conformer. The quasi-axial N−Me ^{13}C NMR signals of **Me$_4$DAB**Pt(d(G*pG*)) adducts are upfield relative to the quasi-equatorial N−Me ^{13}C NMR signals. The same pattern was also observed for **Me$_4$DAB**Pt**G$_2$** adducts.[30] Thus, except as noted next regarding base canting, the macrocyclic ring and the carrier ligand do not interact so strongly as to significantly influence the structure of each other.

Carrier-Ligand Effects on G* Base Canting of HH1 and HH2 Conformers. After the HH or HT orientation of the guanine bases, canting is the second most significant parameter involving the bases and defining the structure of the macrocycle. In most adducts, which usually have relatively small carrier ligands, the bases do not lie exactly perpendicular to the coordination plane. The degree and direction (L or R) of canting (Figure 1) depend on the carrier ligand, on the presence or absence of a linkage between the bases, on the presence or absence of a flanking residue, and even on the single-stranded or duplex character of the DNA. As mentioned above, the degree and direction of canting help to define the distortion in DNA caused by cisplatin-DNA adduct formation. Thus, canting is an important structural feature expected to influence biological activity.

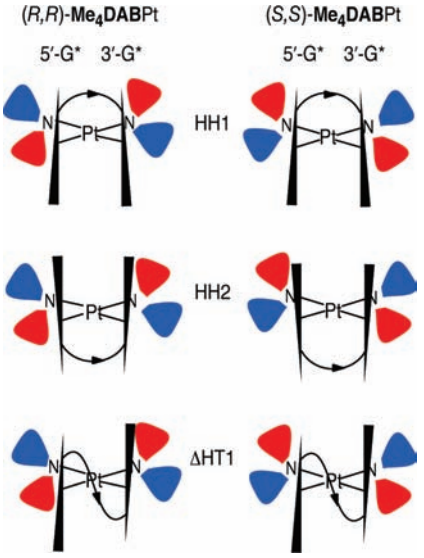

Figure 9. Schematic representation of base orientations for **Me$_4$DAB**Pt(d(G*pG*)) HH1, HH2, and ΔHT1 conformers. G* bases are shown as black triangles with five- and six-membered rings at the tip and base, respectively. Blue (equatorial) and red (axial) areas represent out-of-plane bulk for the carrier ligand).

For adducts with two cis guanines, the H8 shifts reflect the relationship of the H8 of one guanine to the ring current of the cis guanine. Normally, differences in canting influence the shift, but below we introduce a new explanation for the H8 shifts of the ΔHT1 conformer. Typically, H8 signals for clearly canted and less canted bases of HH conformers of both linked and unlinked adducts have chemical shifts from ∼7.8 to 8.3 ppm and ∼8.7 to 9.2 ppm, respectively.[44,49] For a canted G* base, H8 experiences the upfield-shifting effect of the ring-current anisotropy of the cis G* base.[74] In a less canted base, the H8 atom is positioned away from the cis G* base and closer to the perpendicular *z* axis of the complex; as a result, the H8 atom may possibly be deshielded by the Pt magnetic anisotropy.[46,75−77] However, other factors also come into play. In Pt(d(G*pG*)) adducts, an ∼0.3 ppm downfield shift of the 3′-G* H8 atom caused by 3′-G* 5′-phosphate group deshielding is important.[25,44] For example, the two G* H8 signals differ by ∼1.2 ppm for the HH1 conformer of the (*S*,*R*,*R*,*S*)-**Bip**Pt(d(G*pG*)) adduct, which has a clearly canted 5′-G* (shift ≈ 8 ppm) and a less canted 3′-G* base (shift ≈ 9.2 ppm).[44,45,49] For an HH1 conformer, such NMR data suggest for uncanted G* bases H8 shifts of 8.8 (5′-G*) and 9.2 ppm (3′-G*) and for canted G* bases H8 shifts of 7.9 (5′-G*) and 8.2 ppm (3′-G*). Minor factors, such as carrier-ligand influence on solvation and on the inductive effect of the Pt(II) center, lead to 0.1−0.2 ppm variations in these values.

Because there are N−Me groups on both sides of the coordination plane, any base canting for **Me$_4$DAB**Pt(d(G*pG*)) adducts will cause steric clashes between the N−Me groups and the G* H8, O6, C5, and C6 atoms (Figure 9). Indeed, the HH1 conformers for the two **Me$_4$DAB**Pt(d(G*pG*)) adducts have the most downfield 5′-G* and 3′-G* H8 signals (Table 1) observed for a *cis*-PtA$_2$(d(G*pG*)) adduct. The more upfield of the two H8 signals (for 5′-G* in an HH1 conformer) has a relatively downfield shift of

dx.doi.org/10.1021/ic200259s |*Inorg. Chem.* 2011, 50, 4559–4571

~8.6 ppm for both adducts. This shift, which is closer to ~8.8 ppm for a less canted 5′-G* than to the ~7.9 ppm shift for a canted 5′-G*, indicates that the 5′-G* base is at most only slightly canted.

For (*R,R*)-**Me$_4$DAB**Pt(d(G*pG*)), the HH2 H8 shifts (8.95 and 8.80 ppm) are slightly more downfield than the respective shifts (8.71 and 8.78 ppm) for the **Me$_2$ppz**Pt((dG*pG*)) HH2 conformer.[46] The downfield position and the very small difference in these H8 shifts indicate nearly uncanted bases for the HH2 conformers, especially for the (*R,R*)-**Me$_4$DAB**Pt(d(G*pG*)) adduct. As mentioned above, HH conformers require that the H8, O6, C5, and C6 atoms of one G* are near and hence will clash with one of the cis N−Me groups, regardless of the direction of canting. Thus, canting is not favored. The H8 signal for the more canted base of both HH conformers of the **Bip**Pt(d(G*pG*)) adduct underwent a greater upfield shift (~0.5 ppm) between pH ≈ 4 and 10 than the less canted base;[45] this finding is consistent with greater base canting to facilitate carrier-ligand NH group−G* O6 hydrogen bonds after G* N1H deprotonation. In comparison, upfield H8 shift changes of the HH1 conformer for both **Me$_4$DAB**Pt(d(G*pG*)) adducts were less pronounced (~0.15 ppm) when the pH was increased (Supporting Information). The small shifts can be attributed to inductive effects and to at best a very small change in canting. Likewise, the G* H8 signals for the **Me$_2$ppz**Pt(d(G*pG*)) HH1 conformer exhibited small upfield shifts (~0.2−0.3 ppm) as the pH was increased from ~4 to ~10.[46] Thus, for a base to be significantly canted in an HH conformer, the cis amine must have an NH group on the same side of the coordination sphere as the G* O6. In such situations, the low NH steric bulk would not impede the base canting. A relatively upfield H8 shift at a G* residue appears to be closely associated with the guanine O6 being able to form a hydrogen bond with a carrier-ligand NH group.

ΔHT1 Conformer and H8 Shifts. In contrast to the behavior of HH conformers, formation of the Pt−N7 bonds in the ΔHT1 conformer for all *cis*-PtA$_2$(d(G*pG*)) adducts does not shift any H8 signal significantly downfield relative to those of free d(GpG). As mentioned in the Results section, the new results in this study indicate quite clearly that the upfield shift position characteristic of the H8 signal of the ΔHT1 conformer of the two **Me$_4$DAB**Pt((dG*pG*)) adducts cannot result entirely from an increase in shielding from the anisotropic ring current arising from base canting. For reasons described below, we believe that upfield-shifting terms (which in effect cancel the inductive deshielding effect of the Pt) arise from a distortion of the Pt((dG*pG*)) macrocyclic ring.

To describe our reasoning, we turn first to the *cis*-PtA$_2$**G**$_2$ model systems, because the HT conformers are C_2 symmetric and because a sugar phosphate backbone is not present to affect the Δ or Λ chirality of the HT conformer or to restrict the guanine base position. (Note, however, that conformations of *cis*-PtA$_2$**G**$_2$ adducts are subject to other interactions not possible in linked systems, see ref 15.) In **Me$_4$DAB**Pt**G**$_2$ and closely related Pt(*N,N,N′,N′*-tetramethyldiamine)**G**$_2$ model systems, the more stable HT conformer (Δ or Λ) was twice as abundant as the less stable HT conformer (Λ or Δ).[30,50] The more stable HT conformer has **G** H8 (5-membered ring) on the same side of the coordination plane as the quasi-axial N−Me group of the cis amine group.[30,50] One possible explanation is that the positive end of the **G** electric dipole (close to H8) is attracted to the negative end of the cis **G** electric dipole (close to O6). The favored canting direction to maximize this interaction is likely to favor rotation about the Pt−N7 bond such as to move the guanine 5-membered ring toward the cis amine. The H8 N−Me group repulsion with the more distant quasi-axial N−Me groups is likely to be smaller than with the closer quasi-equatorial N−Me groups, accounting for the 2:1 ratio of the HT conformers. Regardless of the specific interaction that influences this equilibrium position, the difference in energy of the interactions must be small for the difference in abundance of the HT conformers to be small. In support of this conclusion, the **G** H8 shifts (which depend on canting) are almost identical for all four HT conformers of both **Me$_4$DAB**Pt**G**$_2$ adducts.[30] Thus, the **Me$_4$DAB** chirality does not significantly influence the structure or the extent of the relatively low degree of canting of the HT conformers. For all **Me$_4$DAB**Pt**G**$_2$ and Pt(*N,N,N′,N′*-tetramethyldiamine)**G**$_2$ adducts, no HH conformer has been observed. The O6 to O6 (cis **G**) repulsion would be so large as to position the guanine bases such that O6 clashes with the N−Me groups would be too large for a detectable amount of the HH conformer to exist. Stated differently, the spatial footprint of an HH conformer is greater than that of an HT conformer.

For the (*S,S*)-**Me$_4$DAB**Pt((dG*pG*)) ΔHT1 conformer, the G* H8 atoms are on the same side of the coordination plane as the quasi-axial N−Me groups, while for the corresponding *R,R* adduct, the G* H8 atoms are on the same side of the coordination plane as the quasi-equatorial N−Me groups. As a result, one might expect a greater degree of canting such as to move the H8 toward the cis amine more for the (*S,S*)-**Me$_4$DAB**Pt((dG*pG*)) adduct than for the *R,R* analogue. However, the very similar G* H8 shifts for the (*S,S*)-**Me$_4$DAB**Pt((dG*pG*)) and (*R,R*)-**Me$_4$DAB**Pt((dG*pG*)) adducts (Table 1) indicate that the ΔHT1 conformer for the *S,S* adduct has a structure and canting very similar to that of the *R,R* adduct. Thus, we conclude that the structure of the ΔHT1 conformer is similar for the *S,S* and *R,R* adducts regardless of the axial/equatorial nature of the N−Me group adjacent to the G* H8, O6, C5, and C6 atoms. We also conclude that the energy differences between these nonbonded interactions are not sufficient to influence the structure of the d(G*pG*) moiety in the ΔHT1 conformers, supporting the view that the spatial footprint of this moiety is small in the ΔHT1 conformers.

As mentioned above, carrier-ligand NH group−G O6 hydrogen bonds are stronger after G* N1H deprotonation; however, such hydrogen bonding requires the G* O6 to be positioned toward the cis amine (as in the case of the *canted* G* base in the HH conformers). The presence of a carrier-ligand NH group hypothetically could lead to a hydrogen bond in the ΔHT1 conformer of the (*S,R,R,S*)-**Bip**Pt(d(G*pG*)) adduct, but such a hydrogen bond is not possible in the ΔHT1 conformer of the **Me$_2$ppz**Pt(d(G*pG*)) adduct.[46,49] However, the similarity of the relatively small upfield shift changes on increasing the pH observed for the ΔHT1 H8 signals of these two adducts indicates that the shifts simply reflect G* N1H deprotonation rather than increases in canting. These results suggest that (a) G* base positioning for the ΔHT1 conformer is not influenced by carrier-ligand to G* O6 hydrogen bonds but is governed by the Pt(d(G*pG*)) ring itself, and (b) even in the deprotonated form of the ΔHT1 conformer of the (*S,R,R,S*)-**Bip**Pt(d(G*pG*)) adduct carrier-ligand to G* O6 hydrogen bonds either are not present or are very weak. This interpretation is also supported by the observation that G* N1H deprotonation at high pH increases the stability of the ΔHT1 conformer of both the (*S,R,R,S*)-**Bip**Pt(d(G*pG*)) and the **Me$_2$ppz**Pt(d(G*pG*)) adducts.[46,49]

Taken together, the evidence at both low and high pH suggests that no significant canting is possible for any **Me$_4$DAB**Pt(d(G*pG*))

conformer. The relatively upfield H8 shifts for the ΔHT1 conformer of **Me$_4$DAB**Pt(d(G*pG*)) adducts strongly indicate that the upfield shifts of H8 signals characteristic of the ΔHT1 conformer of all *cis*-PtA$_2$(d(G*pG*)) adducts are not indicative of canting, even for cases in which the carrier ligand is not bulky. Thus, upfield shifts suggest canting only for HH conformers; such upfield H8 shifts are found for HH conformers only when the carrier ligand has little bulk, as in the cases when an NH group is present. Furthermore, the upfield position of the H8 signals of the ΔHT1 conformer in all *cis*-PtA$_2$(d(G*pG*)) adducts is caused by structural features of a very distorted macrocyclic ring, possibly because the bases are held in close proximity by the distorted macrocyclic ring structure.

Factors Influencing Conformer Distribution. The unusually high abundance of the ΔHT1 conformer for **Me$_4$DAB**Pt(d(G*pG*)) adducts is an important result that emerges from this work. This abundance is higher than for any of the previously studied cross-link adducts.[45,46,49] HH1 and ΔHT1 conformers were observed for (*S*,*S*)-**Me$_4$DAB**Pt(d(G*pG*)); however, three conformers (HH1, HH2, and ΔHT1) were observed for the respective *R*,*R* adduct. The different conformers of the cross-linked models with the two different **Me$_4$DAB** configurations demonstrate that the stereochemistry of the carrier ligand influences which conformers are formed and favored. It is likely that the influence of the **Me$_4$DAB** chelate on the conformer distribution arises from steric effects. However, the structure of the ΔHT1 conformer is similar for the two **Me$_4$DAB**Pt(d(G*pG*)) adducts (as mentioned above).

The ΔHT1:HH1 ratio of conformers for (*S*,*S*)-**Me$_4$DAB**Pt(d(G*pG*)) requires only a 0.4 kcal mol^{-1} free energy difference between conformers favoring the ΔHT1 conformer. The HH1:ΔHT1 ratio of conformers for (*R*,*R*)-**Me$_4$DAB**Pt(d(G*pG*)) suggests a 0.2 kcal mol^{-1} free energy difference favoring the HH1 conformer. For (*S*,*R*,*R*,*S*)-**Bip**Pt(d(G*pG*)), the HH1:ΔHT1 ratio suggests a 0.4 kcal mol^{-1} free energy difference favoring the HH1 conformer.

For only one reported adduct, (*R*,*S*,*S*,*R*)-**Bip**Pt(d(G*pG*)), was no significant amount of the ΔHT1 conformer found, indicating that it is energetically unfavorable.[44] The HH1 and HH2 conformers of this adduct existed in equal abundance and are stabilized by NH to G* O6 H-bonding (3′-G* in HH1 and 5′-G* in HH2). The right-handed canting stabilizes the HH2 conformer, which is ordinarily less stable than the HH1 conformer. All these observations are consistent with the conclusion that, except in an unusual adduct, the presence of the ΔHT1 conformer is to be expected.

Furthermore, a comparison of the results for the ΔHT1 conformer for (*S*,*R*,*R*,*S*)-**Bip**Pt(d(G*pG*)), **Me$_2$ppz**Pt(d(G*pG*)), and **Me$_4$DAB**Pt(d(G*pG*)) adducts establishes that carrier-ligand NH to G* O6 hydrogen bonding has no influence on base canting (similar H8 shifts) and is not a significant stabilizing factor. The order of relative stability of the ΔHT1 conformer [(*S*,*S*)-**Me$_4$DAB**Pt(d(G*pG*)) > (*R*,*R*)-**Me$_4$DAB**Pt(d(G*pG*)) ≈ (*S*,*R*,*R*,*S*)-**Bip**Pt(d(G*pG*)) ≈ **Me$_2$ppz**Pt(d(G*pG*)) > (*R*,*S*,*S*,*R*)-**Bip**Pt(d(G*pG*))] trends with decreasing carrier-ligand steric bulk and inversely with the likely presence of canted, hydrogen-bonded G* bases in HH conformers.

We believe that the common conformations of the Pt(d(G*pG*)) macrocyclic ring (HH1, HH2, ΔHT1) must be relatively similar in energy for conditions in which the two G*'s have N1H in the normal protonation state. Upon G* N1H deprotonation (pH > 10), the ΔHT1 conformer of **Me$_4$DAB**Pt(d(G*pG*)) adducts becomes unusually highly favored (up to ∼88% of the total conformer distribution). Likewise, an increase in abundance of the ΔHT1 conformer at pH ≈ 10 was also observed for **Me$_2$ppz**Pt(d(G*pG*)).[46] Because the **Me$_2$ppz** ligand lacks NH groups, amine to G* O6 hydrogen bonding is not present for **Me$_2$ppz**Pt(d(G*pG*)). Thus, the increase in abundance of the ΔHT1 conformer upon G* N1H deprotonation for all adducts is strong evidence that the stability of the ΔHT1 conformer of *cis*-PtA$_2$(d(G*pG*)) adducts arises almost exclusively from forces within the Pt(d(G*pG*)) macrocycle and depends little on any interactions between the carrier ligand and the dinucleotide. G* N1H deprotonation may increase the (base dipole)−(base dipole) interaction that favors the HT arrangement. All results indicate that the carrier-ligand NH to G* O6 hydrogen bonding is not important in favoring the ΔHT1 conformer. The (base dipole)−(base dipole) interaction at high pH is favorable in the ΔHT1 conformer but is very unfavorable for the HH conformers, especially when the degree of base canting is low. Thus, the HH1 conformer of **Me$_4$DAB**Pt(d(G*pG*)) adducts becomes less stable upon G* N1H deprotonation. Indeed, the effect seems even greater on the HH2 conformer. Interestingly, at high pH, the HH2 conformer is nonexistent for (*R*,*R*)-**Me$_4$DAB**Pt(d(G*pG*)) and **Me$_2$ppz**Pt(d(G*pG*))[46] adducts, indicating particularly unfavorable base−base interactions in this conformer when the bases are deprotonated.

CONCLUSIONS

Several new findings from this first detailed study of Pt−DNA cross-link adducts with a carrier ligand possessing significant bulk lead to a number of new conclusions and expand or support conclusions reached in previous studies as follows.

(i) The crowded environment of the **Me$_4$DAB** ligand, which precludes significant base canting, favors formation of the ΔHT1 conformer. This study of the **Me$_4$DAB**Pt(d(G*pG*)) adducts provides for the first time compelling evidence that the ΔHT1 conformer has an unusually distorted structure with essentially uncanted bases. Unusual ^{31}P and ^{13}C NMR shifts support this conclusion. Regardless of carrier-ligand bulk or hydrogen-bonding potential, the ΔHT1 conformers for all adducts have similar relatively upfield H8 and ^{31}P NMR signals and thus nearly identical Pt(d(G*pG*)) macrocyclic rings. The upfield H8 shifts can now be confidently attributed to mutual shielding by the cis guanine base anisotropy as a result of the base proximity in the unusual structure rather than to base canting in the ΔHT1 conformers.

(ii) The corresponding HH1 and ΔHT1 conformers of the (*S*,*S*)- and (*R*,*R*)-**Me$_4$DAB**Pt(d(G*pG*)) adducts have almost identical NMR parameters, but the relative stability of the conformers differs in the two adducts. We conclude that the differences in the **Me$_4$DAB** ligand interactions with the guanine bases resulting from the difference in **Me$_4$DAB** chirality are not sufficient to change structure but are sufficient to modify slightly the distribution of conformers.

(iii) Both (*R*,*R*)- and (*S*,*S*)-**Me$_4$DAB**Pt(d(G*pG*)) have a substantial HH1 conformer abundance, mirroring the abundance found in several adducts with much less sterically hindering environments.[11,44,46] The sugar-phosphate backbone thus has sufficient influence to overcome the base−base interactions that normally preclude the existence of HH conformers in adducts with sterically hindering *N*,*N*,*N*′,*N*′-tetramethyldiamine carrier ligands.

dx.doi.org/10.1021/ic200259s |*Inorg. Chem.* 2011, 50, 4559–4571

(iv) We conclude that the energy difference between the commonly observed abundant *cis*-PtA_2(d(G*pG*)) conformers (HH1, HH2, and ΔHT1) is inherently small, with the backbone slightly favoring the HH1 conformer. Normally the carrier-ligand interactions with the guanine bases merely modulate the relative abundance of these conformers.

(v) The order of relative stability of the ΔHT1 conformer for multiple adducts establishes that carrier-ligand NH to G* O6 hydrogen bonding is not a significant stabilizing interaction. The absence of such an effect is consistent with a relatively low degree of base canting in all of the ΔHT1 conformers because canting is needed in order for NH to G* O6 hydrogen bonding to occur.

(vi) The ΔHT1 conformer for **Me_4DAB**Pt(d(G*pG*)) adducts was found in exceptionally high abundance after G* N1H deprotonation (up to 88%), the highest such abundance ever observed for a cross-link adduct. Destabilization of the HH1 conformer and stabilization of the ΔHT1 conformer are caused by the better (base dipole)−(base dipole) interaction favoring HT over HH conformers. Upon G* N1H deprotonation, the G* $N1^-$ to G* $N1^-$ repulsion in an HT conformer is minimal because of the long distance between the ends of the G* bases. Because of this factor, a substantial amount of the less favored ΛHT2 conformer was observed at basic pH for the (*R*,*R*)-**Me_4DAB**Pt(d(G*pG*)) adduct.

Finally, the present findings raise the possibility that the high toxicity[33,78] and low activity of the bulky analogues of cisplatin may originate from the formation of less of the usually abundant HH1 conformer, the predominant conformation that is adopted by the major lesion in cisplatin−DNA adducts. Our studies show that this conformer does form but that base canting is negligible. Studies employing longer oligonucleotides may reveal how the N-alkyl groups interact with flanking residues and influence base canting in DNA adducts.

■ ASSOCIATED CONTENT

Supporting Information. Description of ^{1}H and ^{13}C NMR assignments for the ΛHT2 conformer; H8 and ^{31}P NMR shifts and conformer distribution of **Me_4DAB**Pt(d(G*pG*)) adducts as a function of pH; ^{1}H, ^{13}C, and ^{31}P NMR shifts for the (*R*,*R*)-**Me_4DAB**Pt(d(G*pG*)) adduct at pH 10.3; ^{1}H and ^{13}C NMR shifts for N−Me groups of **Me_4DAB**Pt(d(G*pG*)) adducts; ^{1}H and ^{13}C NMR assignments of free d(GpG); schematic representation of the ΔHT1 and ΛHT2 conformers of the (*R*,*R*)-**Me_4DAB**Pt(d(G*pG*)) adduct; ^{31}P, ROESY, and HMQC NMR spectra of **Me_4DAB**Pt(d(G*pG*)) adducts. This material is available free of charge via the Internet at http://pubs.acs.org.

■ AUTHOR INFORMATION

Corresponding Author

*E-mail: lmarzil@lsu.edu (L.G.M.), saad@uab.edu (J.S.S.).

Present Addresses

[‡]Department of Microbiology, University of Alabama at Birmingham, 845 19th Street South, Birmingham, Alabama 35294.

[∥]Dipartimento di Scienze e Tecnologie Biologiche ed Ambientali, Università del Salento, Via Provinciale Lecce-Monteroni, 73100 Lecce, Italy

■ ACKNOWLEDGMENT

This investigation was supported by the UAB Comprehensive Cancer Center (to J.S.S.), by LSU (to L.G.M.), and by EC (COST Action D39) and the University of Bari (to G.N.). We thank Dr. Patricia Marzilli (LSU) for useful discussions and suggestions regarding this work.

■ REFERENCES

(1) Arnesano, F.; Natile, G. *Coord. Chem. Rev.* **2009**, *253*, 2070–2081.
(2) Centerwall, C. R.; Goodisman, J.; Kerwood, D. J.; Dabrowiak, J. C. *J. Am. Chem. Soc.* **2005**, *127*, 12768–12769.
(3) Decatris, M. P.; Sundar, S.; O'Byrne, K. J. *Cancer Treat. Rev.* **2004**, *30*, 53–81.
(4) Jakupec, M. A.; Galanski, M.; Arion, V. B.; Hartinger, C. G.; Keppler, B. K. *Dalton Trans.* **2008**, 183–194.
(5) Kelland, L. *Nat. Rev. Cancer* **2007**, *7*, 573–584.
(6) Klein, A. V.; Hambley, T. W. *Chem. Rev.* **2009**, *109*, 4911–4920.
(7) Lippert, B. *Cisplatin. Chemistry and Biochemistry of a Leading Anticancer Drug*; Wiley-VCH: Weinheim, 1999.
(8) Reedijk, J. *Eur. J. Inorg. Chem.* **2009**, *10*, 1303–1312.
(9) Wang, D.; Lippard, S. J. *Nat. Rev. Drug Discovery* **2005**, *4*, 307–320.
(10) Beljanski, V.; Villanueva, J. M.; Doetsch, P. W.; Natile, G.; Marzilli, L. G. *J. Am. Chem. Soc.* **2005**, *127*, 15833–15842.
(11) Bhattacharyya, D.; Marzilli, P. A.; Marzilli, L. G. *Inorg. Chem.* **2005**, *44*, 7644–7651.
(12) Chaney, S. G.; Campbell, S. L.; Temple, B.; Bassett, E.; Wu, Y.; Faldu, M. *J. Inorg. Biochem.* **2004**, *98*, 1551–1559.
(13) Kaspárková, J.; Vojtiskova, M.; Natile, G.; Brabec, V. *Chem.—Eur. J.* **2008**, *14*, 1330–1341.
(14) Malina, J.; Novakova, O.; Vojtiskova, M.; Natile, G.; Brabec, V. *Biophys. J.* **2007**, *93*, 3950–3962.
(15) Natile, G.; Marzilli, L. G. *Coord. Chem. Rev.* **2006**, *250*, 1315–1331.
(16) Ober, M.; Lippard, S. J. *J. Am. Chem. Soc.* **2008**, *130*, 2851–2861.
(17) Ohndorf, U.-M.; Lippard, S. J. In *DNA Damage Recognition*; Siede, W., Kow, Y. W., Doetsch, P. W., Eds.; CRC: London, 2006; Vol. 12, pp 239−261.
(18) Sherman, S. E.; Gibson, D.; Wang, A.; Lippard, S. J. *J. Am. Chem. Soc.* **1988**, *110*, 7368–7381.
(19) Sherman, S. E.; Gibson, D.; Wang, A. H.-J.; Lippard, S. J. *Science* **1985**, *230*, 412–417.
(20) Ano, S. O.; Kuklenyik, Z.; Marzilli, L. G. In *Cisplatin. Chemistry and Biochemistry of a Leading Anticancer Drug*; Lippert, B., Ed.; Wiley-VCH: Basel, 1999; pp 247−291.
(21) Marzilli, L. G.; Saad, J. S.; Kuklenyik, Z.; Keating, K. A.; Xu, Y. *J. Am. Chem. Soc.* **2001**, *123*, 2764–2770.
(22) Ohndorf, U.-M.; Rould, M. A.; He, Q.; Pabo, C. O.; Lippard, S. J. *Nature* **1999**, *399*, 708–712.
(23) Lovejoy, K. S.; Todd, R. C.; Zhang, S.; McCormick, M. S.; D'Aquino, J. A.; Reardon, J. T.; Sancar, A.; Giacomini, K. M.; Lippard, S. J. *Proc. Natl. Acad. Sci. U.S.A.* **2008**, *105*, 8902–8907.
(24) Todd, R. C.; Lippard, S. J. In *Platinum and Other Heavy Metal Compounds in Cancer Chemotherapy*; Bonetti, A., Leone, R., Muggia, F. M., Howell, S. B., Eds.; Humana Press: Totowa, NJ, 2009; pp 67−72.
(25) Saad, J. S.; Natile, G.; Marzilli, L. G. *J. Am. Chem. Soc.* **2009**, *131*, 12314–12324.
(26) Hambley, T. W. *Coord. Chem. Rev.* **1997**, *166*, 181–223.
(27) Haxton, K. J.; Burt, H. M. *J. Pharm. Sci.* **2009**, *98*, 2299–2316.
(28) Benedetti, M.; Malina, J.; Kaspárková, J.; Brabec, V.; Natile, G. *Environ. Health Perspect.* **2002**, *110*, 779–782.
(29) Orbell, J. D.; Taylor, M. R.; Birch, S. L.; Lawton, S. E.; Vilkins, L. M.; Keefe, L. J. *Inorg. Chim. Acta* **1988**, *152*, 125–134.
(30) Saad, J. S.; Benedetti, M.; Natile, G.; Marzilli, L. G. *Inorg. Chem.* **2010**, *49*, 5573–5583.
(31) Milanesio, M.; Monti, E.; Gariboldi, M. B.; Gabano, E.; Ravera, M.; Osella, D. *Inorg. Chim. Acta* **2008**, *361*, 2803–2814.

(32) Cramer, R. E.; Dahlstrom, P. L. *J. Am. Chem. Soc.* **1979**, *101*, 3679–3681.
(33) Hirano, T.; Inagaki, K.; Fukai, T.; Alink, M.; Nakahara, H.; Kidani, Y. *Chem. Pharm. Bull.* **1990**, *38*, 2850–2852.
(34) Bloemink, M. J.; Reedijk, J. In *Metal Ions in Biological Systems*; Sigel, A., Sigel, H., Eds.; Marcel Dekker, Inc.: New York, 1996; Vol. 32, pp 641−685.
(35) Sherman, S. E.; Lippard, S. J. *Chem. Rev.* **1987**, *87*, 1153–1181.
(36) Ano, S. O.; Intini, F. P.; Natile, G.; Marzilli, L. G. *J. Am. Chem. Soc.* **1997**, *119*, 8570–8571.
(37) Ano, S. O.; Intini, F. P.; Natile, G.; Marzilli, L. G. *Inorg. Chem.* **1999**, *38*, 2989–2999.
(38) Kiser, D.; Intini, F. P.; Xu, Y.; Natile, G.; Marzilli, L. G. *Inorg. Chem.* **1994**, *33*, 4149–4158.
(39) Marzilli, L. G.; Intini, F. P.; Kiser, D.; Wong, H. C.; Ano, S. O.; Marzilli, P. A.; Natile, G. *Inorg. Chem.* **1998**, *37*, 6898–6905.
(40) Saad, J. S.; Scarcia, T.; Natile, G.; Marzilli, L. G. *Inorg. Chem.* **2002**, *41*, 4923–4935.
(41) Xu, Y.; Natile, G.; Intini, F. P.; Marzilli, L. G. *J. Am. Chem. Soc.* **1990**, *112*, 8177–8179.
(42) Saad, J. S.; Scarcia, T.; Shinozuka, K.; Natile, G.; Marzilli, L. G. *Inorg. Chem.* **2002**, *41*, 546–557.
(43) Sullivan, S. T.; Ciccarese, A.; Fanizzi, F. P.; Marzilli, L. G. *Inorg. Chem.* **2001**, *40*, 455–462.
(44) Ano, S. O.; Intini, F. P.; Natile, G.; Marzilli, L. G. *J. Am. Chem. Soc.* **1998**, *120*, 12017–12022.
(45) Williams, K. M.; Cerasino, L.; Natile, G.; Marzilli, L. G. *J. Am. Chem. Soc.* **2000**, *122*, 8021–8030.
(46) Sullivan, S. T.; Ciccarese, A.; Fanizzi, F. P.; Marzilli, L. G. *J. Am. Chem. Soc.* **2001**, *123*, 9345–9355.
(47) Sullivan, S. T.; Ciccarese, A.; Fanizzi, F. P.; Marzilli, L. G. *Inorg. Chem.* **2000**, *39*, 836–842.
(48) Cramer, R.; Dahlstrom, P. *Inorg. Chem.* **1985**, *24*, 3420–3424.
(49) Marzilli, L. G.; Ano, S. O.; Intini, F. P.; Natile, G. *J. Am. Chem. Soc.* **1999**, *121*, 9133–9142.
(50) Benedetti, M.; Saad, J. S.; Marzilli, L. G.; Natile, G. *J. Chem. Soc., Dalton Trans.* **2003**, 872–879.
(51) Dijt, F. J.; Canters, G. W.; den Hartog, J. H.; Marcelis, A.; Reedijk, J. *J. Am. Chem. Soc.* **1984**, *106*, 3644–3647.
(52) Qu, Y.; Farrell, N. *J. Am. Chem. Soc.* **1991**, *113*, 4851–4857.
(53) Delaglio, F.; Grzesiek, S.; Vuister, G. W.; Zhu, G.; Pfeifer, J.; Bax, A. *J. Biomol. NMR* **1995**, *6*, 277–293.
(54) Johnson, B. A.; Blevins, R. A. *J. Biomol. NMR* **1994**, *4*, 603–614.
(55) Berners-Price, S. J.; Ranford, J. D.; Sadler, P. J. *Inorg. Chem.* **1994**, *33*, 5842–5846.
(56) den Hartog, J. H. J.; Altona, C.; Chottard, J.-C.; Girault, J.-P.; Lallemand, J.-Y.; de Leeuw, F. A.; Marcelis, A. T. M.; Reedijk, J. *Nucleic Acids Res.* **1982**, *10*, 4715–4730.
(57) den Hartog, J. H. J.; Altona, C.; van der Marel, G. A.; Reedijk, J. *Eur. J. Biochem.* **1985**, *147*, 371–379.
(58) Girault, J.-P.; Chottard, G.; Lallemand, J.-Y.; Chottard, J.-C. *Biochemistry* **1982**, *21*, 1352–1356.
(59) Mukundan, S., Jr.; Xu, Y.; Zon, G.; Marzilli, L. G. *J. Am. Chem. Soc.* **1991**, *113*, 3021–3027.
(60) van der Veer, J. L.; van der Marel, G. A.; van den Elst, H.; Reedijk, J. *Inorg. Chem.* **1987**, *26*, 2272–2275.
(61) Wüthrich, K. *NMR of Proteins and Nucleic Acids*; John Wiley & Sons: New York, 1986.
(62) Saenger, W. *Principles of Nucleic Acid Structure*; Springer-Verlag: New York, 1984.
(63) Patel, D. J.; Kozlowski, S. A.; Nordheim, A.; Rich, A. *Proc. Natl. Acad. Sci. U.S.A.* **1982**, *79*, 1413–1417.
(64) Kaspárková, J.; Mellish, K. J.; Qu, Y.; Brabec, V.; Farrell, N. *Biochemistry* **1996**, *35*, 16705–16713.
(65) Yang, D.; van Boom, S.; Reedijk, J.; van Boom, J.; Wang, A. *Biochemistry* **1995**, *34*, 12912–12920.
(66) Iwamoto, M.; Mukundan, S., Jr.; Marzilli, L. G. *J. Am. Chem. Soc.* **1994**, *116*, 6238–6244.
(67) Wang, Y.; de los Santos, C.; Gao, X.; Greene, K. L.; Live, D. H.; Patel, D. J. *J. Mol. Biol.* **1991**, *222*, 819–832.
(68) Booth, H.; Everett, J. R.; Fleming, R. A. *Org. Magn. Reson.* **1979**, *12*, 63–66.
(69) Bancroft, D. P.; Lepre, C. A.; Lippard, S. J. *J. Am. Chem. Soc.* **1990**, *112*, 6860–6871.
(70) Miller, S. K.; Marzilli, L. G. *Inorg. Chem.* **1985**, *24*, 2421–2425.
(71) Marzilli, L. G.; Hayden, Y.; Reily, M. D. *Inorg. Chem.* **1986**, *25*, 974–978.
(72) Benedetti, M.; Tamasi, G.; Cini, R.; Natile, G. *Chem.—Eur. J.* **2003**, *9*, 6122–6132.
(73) Sullivan, S. T.; Saad, J. S.; Fanizzi, F. P.; Marzilli, L. G. *J. Am. Chem. Soc.* **2002**, *124*, 1558–1559.
(74) Kozelka, J.; Fouchet, M. H.; Chottard, J.-C. *Eur. J. Biochem.* **1992**, *205*, 895–906.
(75) Carlone, M.; Fanizzi, F. P.; Intini, F. P.; Margiotta, N.; Marzilli, L. G.; Natile, G. *Inorg. Chem.* **2000**, *39*, 634–641.
(76) Elizondo-Riojas, M.-A.; Kozelka, J. *Inorg. Chim. Acta* **2000**, *297*, 417–420.
(77) Sundquist, W.; Lippard, S. J. *Coord. Chem. Rev.* **1990**, *100*, 293–322.
(78) Bloemink, M. J.; Heetebrij, R. J.; Inagaki, K.; Kidani, Y.; Reedijk, J. *Inorg. Chem.* **1992**, *31*, 4656–4661.